CXCL13/CXCR5 signaling enhances BCR-triggered B-cell activation by shaping cell dynamics

Julia Sáez de Guinoa,[1] Laura Barrio,[1] Mario Mellado,[2] and Yolanda R. Carrasco[1]

[1]B Cell Dynamics Group, Department of Immunology and Oncology, Centro Nacional de Biotecnología/Consejo Superior de Investigaciones Científicas, Madrid, Spain; and [2]Chemokine Signaling Group, Department of Immunology and Oncology, Centro Nacional de Biotecnología/Consejo Superior de Investigaciones Científicas, Madrid, Spain

Continuous migration of B cells at the follicle contrasts with their stable arrest after encounter with antigen. Two main ligand/receptor pairs are involved in these cell behaviors: the chemokine CXCL13/chemokine receptor CXCR5 and antigen/BCR. Little is known regarding the interplay between CXCR5 and BCR signaling in the modulation of B-cell dynamics and its effect on B-cell activation. We used a 2-dimensional model to study B-cell migration and antigen recognition in real time, and found that BCR signaling strength alters CXCL13-mediated migration, leading to a heterogeneous B-cell behavior pattern. In addition, we demonstrate that CXCL13/CXCR5 signaling does not impair BCR-triggered immune synapse formation and that CXCR5 is excluded from the central antigen cluster. CXCL13/CXCR5 signaling enhances BCR-mediated B-cell activation in at least 2 ways: (1) it assists antigen gathering at the synapse by promoting membrane ruffling and lymphocyte function–associated antigen 1 (LFA-1)–supported adhesion, and (2) it allows BCR signaling integration in motile B cells through establishment of LFA-1–supported migratory junctions. Both processes require functional actin cytoskeleton and nonmuscle myosin II motor protein. Therefore, the CXCL13/CXCR5 signaling effect on shaping B-cell dynamics is an effective mechanism that enhances antigen encounter and BCR-triggered B-cell activation. (*Blood.* 2011;118(6):1560-1569)

Introduction

The incessant migration of B cells in vivo in the secondary lymphoid organs (ie, the lymph nodes and spleen) is a search for specific antigens.[1,2] Once B cells enter lymph nodes through the high endothelial venules, they move toward the follicles, guided by the chemokine CXCL13 and a network of stromal cells.[3] B cells concentrate in the proximity of the follicular dendritic cell (FDC) network to form the follicles, which are confined by a ceiling of subcapsular sinus macrophages, a floor of fibroblastic reticular cells and dendritic cells, and interfollicular walls composed mainly of macrophages and fibroblastic reticular cells. In steady-state conditions, B cells explore the entire follicular volume, moving randomly at an average speed of 6 μm/min.[1,2] CXCL13, which is produced mainly by FDCs, underlies this B-cell behavior by signaling through its receptor, CXCR5.[4]

Specific antigen recognition through BCR alters steady-state B-cell dynamics at the follicle. B cells stop to gather antigen into a central cluster at the site of contact with the antigen-presenting cell, establishing an immune synapse (IS).[5] IS formation is critical for B-cell activation, antigen internalization, and affinity discrimination, as shown by in vitro[6,7] and in vivo approaches.[8] Although the B cell IS persists for at least 20-30 minutes, it is a transient stage. In vivo, B cells accumulate particulate antigen with time[5] up to a threshold that triggers their capacity to respond to CCL21 through CCR7, after which they exit the follicle in search of T-cell help.[2] These data suggest a series of "stop plus IS" events, followed by "go or motile" events on the B cell to achieve antigen accumulation. Modulation of B-cell dynamics thus becomes critical for shaping the process of antigen encounter and subsequent B-cell activation. The nature of the interplay between BCR and CXCR5 in regulating B-cell behavior is nonetheless almost entirely unknown.

We established a 2-dimensional model that allows the study of CXCL13-mediated B-cell migration and antigen encounter in real time. To mimic the cell surface, we used planar lipid bilayers containing the lymphocyte function–associated antigen 1 (LFA-1) integrin ligand ICAM-1 as the GPI-linked protein, as well as tethered antigen and a CXCL13 coating. This model allowed us to reproduce steady-state B-cell dynamic parameters similar to those observed in vivo with multiphoton microscopy techniques. Using distinct BCR transgenic models, we show herein that BCR signaling strength alters CXCL13-mediated B-cell migration. CXCL13/CXCR5 signaling does not significantly affect BCR-triggered IS formation, and CXCR5 segregates outside of the central antigen/BCR cluster of the synapse; however, it enhances BCR-mediated cell activation. CXCL13/CXCR5 facilitated antigen encounter and BCR signaling by promoting membrane ruffling and LFA-1–supported adhesion in stopped/IS-forming B cells, and through the establishment of an LFA-1–supported migratory junction ("kinapse") in motile B cells. Both mechanisms require a functional actin cytoskeleton and the activity of the motor protein non-muscle myosin II (NM-II).

Submitted January 21, 2011; accepted May 30, 2011. Prepublished online as *Blood* First Edition paper, June 9, 2011; DOI 10.1182/blood-2011-01-332106.

The online version of this article contains a data supplement.

The publication costs of this article were defrayed in part by page charge payment. Therefore, and solely to indicate this fact, this article is hereby marked "advertisement" in accordance with 18 USC section 1734.

Methods

Mice and cells

Wild-type (C57BL/6, BALB/c) and genetically modified naive B cells (BCR-transgenic and CXCR5-deficient) were freshly isolated from spleens of wild-type, MD4,[9] 3-83,[10] and CXCR5-deficient mice[11] by negative selection (> 95% purity), as described previously.[6] Purified B cells were labeled with 0.1μM CFSE long-term dye (Molecular Probes) for 10 minutes at 37°C before use. Animal experimentation was approved by the Centro Nacional de Biotecnología/Consejo Superior de Investigaciones Científicas Bioethics Committee and conforms to institutional and national regulations. The murine A20 B-cell line was stably transfected with the CXCR5-green fluorescent protein (GFP) construct (see supplemental Methods, available on the *Blood* Web site; see the Supplemental Materials link at the top of the online article).

Time-lapse microscopy on planar lipid bilayers

Planar lipid bilayers were prepared as described previously.[6] Briefly, unlabeled GPI-linked ICAM-1 liposomes and/or liposomes containing biotinylated lipids were mixed with 1,2-dioleoyl-PC at various ratios to obtain specified molecular densities. Membranes were assembled in FCS2 chambers (Bioptechs) and then blocked with PBS with 2% FCS for 1 hour at room temperature. Antigen was tethered by incubating membranes with Alexa Fluor 647–streptavidin (Molecular Probes), followed by monobiotinylated peptide p31 for 3-83 B cells,[12] monobiotinylated F10 anti–hen egg lysozyme (anti-HEL) mAb plus HEL (Sigma-Aldrich) for MD4 B cells,[6] or monobiotinylated anti-κ light chain mAb (BD Biosciences) for non-BCR transgenic B cells and the A20 B-cell line. The final step was coating with recombinant murine CXCL13 (Peprotech) at the indicated concentration for 30 minutes at room temperature immediately before imaging. CFSE-labeled B cells were injected into the warmed (37°C) chamber at time zero; confocal fluorescence, differential interference contrast (DIC), and interference reflection microscopy (IRM) images were acquired every 10 seconds for 25 minutes. All assays were performed in PBS with 0.5% FCS, 0.5 g/L of D-glucose, 2mM $MgCl_2$, and 0.5mM $CaCl_2$, followed by injection with latrunculin A (0.5μM; Calbiochem) or blebbistatin (50μM; Calbiochem) to the FCS2, waiting for 5-10 minutes, and then imaging again for 20 minutes. Images were acquired on a Zeiss Axiovert LSM 510-META inverted microscope with a 40× oil-immersion objective and analyzed by LSM 510 software (Zeiss) and Imaris 6.0 software (Bitplane). Graphs and statistical analyses were generated with Prism 4.0 software (GraphPad); the unpaired Student *t* test was applied. For quantitative studies at the target membrane and the cell surface, see supplemental Methods.

For intracellular Ca^{2+} flux measurement, purified B cells were labeled with 1μM Fluo-4FF (Molecular Probes) for 30 minutes at room temperature, immediately injected into the warmed FCS2 chamber, and imaged every 10 seconds for 15 or 30 minutes at low quality to speed up acquisition. Ca^{2+} flux was monitored by fluorescence and DIC images, and analyzed by LSM 510 software (Zeiss).

Immunofluorescence and B-cell activation assays

For details of the immunofluorescence and B-cell activation assays, please see supplemental Methods.

Results

Two-dimensional model to study B-cell dynamics in response to CXCR5 and BCR signaling

To dissect the control of naive B-cell dynamics by CXCR5 and BCR signaling, we established a model that allowed simultaneous study of CXCL13-mediated B-cell migration, B-cell antigen recognition, and IS formation. The planar lipid bilayer system mimics the fluid surface of a cell[13] and has been used to study B-cell antigen encounter[6]; we optimized conditions for migration of primary naive B cells in response to CXCL13 on this substrate. Data for CXCL13 immunostaining in lymphoid tissue,[14] as well as its ability to bind certain glycosaminoglycans present on cell surfaces,[15] suggest that, in vivo, B cells encounter CXCL13 on the FDC surface; the FDC network has a central role in orchestrating B-cell motility at the follicle.[3] To mimic this in vivo situation, we coated the artificial membranes with CXCL13 and, given the positive charge of chemokines, CXCL13 easily associated with the negatively charged phospholipids through electrostatic interaction. Homogeneous CXCL13 binding to the lipid bilayer might provide a chemokinetic stimulus and thus lead to random B-cell migration, as described in vivo[1,2]; to date, no CXCL13 gradient has been reported within the follicle. As a GPI-linked membrane protein, we included the adhesion molecule ICAM-1, the principal ligand of the integrin LFA-1. LFA-1/ICAM-1 have a critical role in B-cell IS formation,[6] and are implicated in B-cell contact with FDCs[16] and in lymphocyte movement.[17-19] In addition, leukocytes show a preference for migrating on adhesive substrates coated with immobilized chemokine.[20] The setup of our model might therefore promote this type of "haptokinetic" response in B cells.

We isolated wild-type naive B cells from mouse spleen and assayed their migratory capacity on CXCL13-coated, ICAM-1–containing membranes in real time using confocal microscopy approaches (supplemental Video 1). DIC examination of naive B cells on ICAM-1–containing membranes with CXCL13 coating showed 2 distinct morphologies: nonpolarized B cells (round shape) and cells with a flattened leading-edge extension at the front (lamellipodium), followed by the bulky nucleus at the back (polarized B cells; Figure 1A). The presence of CXCL13 on the membrane was sufficient to promote polarization of the naive B-cell population (Figure 1B). Nonetheless, naive B cells migrated only when CXCL13 was combined with ICAM-1. Both CXCL13-mediated cell polarization and migration were dependent on the expression of CXCR5 at the B-cell surface, as the results with CXCR5-deficient B cells indicated (Figure 1B).

Above a minimum ICAM-1 density of 75 molecules/μm^2, most of the B-cell population migrated in response to CXCL13 (Figure 1B). Both cell polarization and migration were dependent on the chemokine concentration used to coat the membranes, and therefore on the amount of CXCL13 on the bilayer (Figure 1C); 100nM CXCL13 yielded optimal B-cell polarization and migratory responses. Analysis of the cell dynamic parameters showed an average speed of > 5 μm/min at ICAM-1 densities of 150 and 300 molecules/μm^2 (Figure 1D), which is very close to the in vivo B-cell interstitial velocity within the follicle (6 μm/min).[1] The tracks stress the characteristic random B-cell motility, with average total lengths of 120 μm for the time recorded (Figure 1D-E). Migration of naive B cells slowed when they were exposed to higher ICAM-1 densities (600 molecules/μm^2; Figure 1D), highlighting the effect of the integrin ligand on B-cell dynamics. We used IRM to analyze the nature of the contacts established by B cells with the lipid bilayer at different ICAM-1 densities (Figure 1F). Migration failure at ICAM-1 densities of < 75 molecules/μm^2 correlated with small, intermittent B-cell contacts. B cell: membrane interactions were similar in area and were stable over time at higher densities.

We established a 2-dimensional model that supports naive B-cell migration in response to CXCL13. The use of 100nM CXCL13 to coat the membrane plus an ICAM-1 density of 150 molecules/μm^2 yielded optimal conditions for B-cell motility,

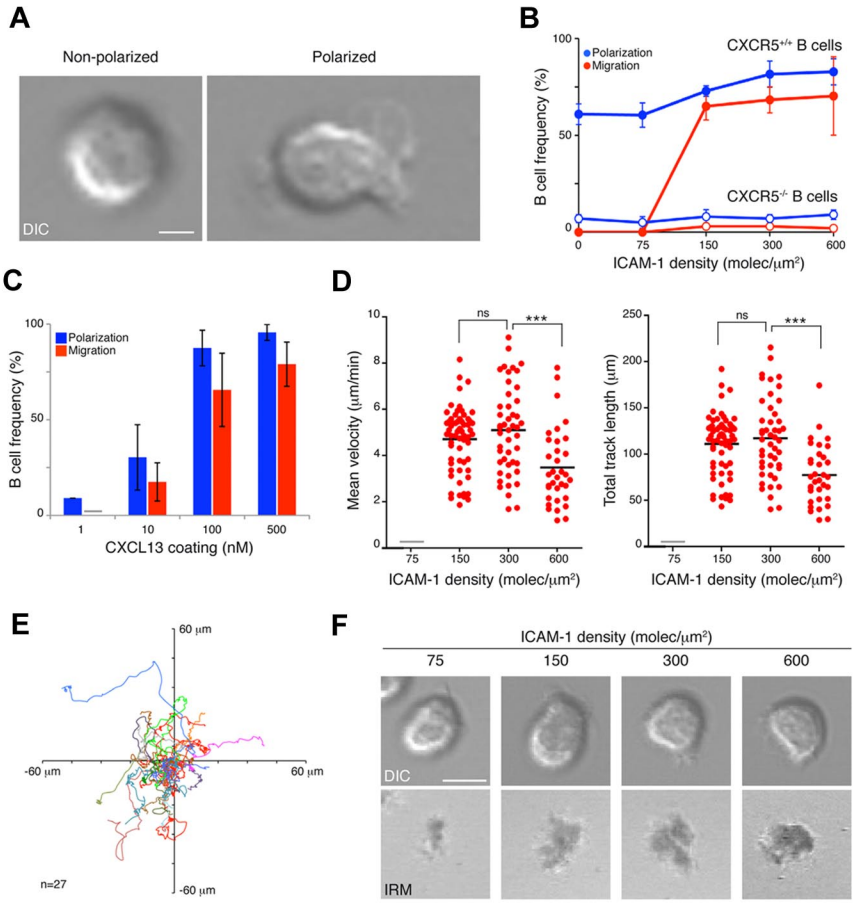

Figure 1. Naive B-cell dynamics on 2-dimensional membranes. (A) DIC images of representative nonpolarized and polarized naive B cells on ICAM-1–containing membranes, coated with 100nM CXCL13. Scale bar indicates 2 μm. (B) Frequency of naive B-cell polarization and migration on membranes containing ICAM-1 at different densities and coated with 100nM CXCL13. Filled symbols indicate wild-type B cells; open symbols, CXCR5-deficient B cells. (C) Frequency of naive B-cell polarization and migration on ICAM-1 (150 molecules/μm²)–containing membranes coated with different concentrations of CXCL13. Values for mean velocity and total track length (D) and tracks of migratory B cells (E) on ICAM-1–containing membranes coated with 100nM CXCL13. (F) Representative DIC and IRM images of naive B cells on ICAM-1–containing membranes at specified densities and CXCL13 coating (100nM). Scale bar indicates 5 μm. Data in panels B and C represent the mean ± SEM of 4 experiments; data in panels D and E correspond to the merge of 3 experiments. Gray bar indicates not detected; ns, not significant. ***$P < .0001$.

and resembled in vivo steady-state dynamics in the follicle. We used these conditions for the remainder of the study.

BCR signaling strength alters CXCL13-mediated B-cell migration

To study the effect of antigen encounter on CXCL13-induced B-cell migration, we used BCR-transgenic 3-83 B cells, which recognize the p31 antigenic peptide with low affinity (K_A 65 × 10^6 M^{-1}). We anchored p31 to the membrane, as described previously[6] (see "Methods"). The dynamic parameters of 3-83 naive B-cell movement across the ICAM-1–containing membranes were equivalent to those of wild-type B cells in response to CXCL13 (Figure 2A-C). Depending on its density, tethered p31 altered cell migration in several ways (Figure 2A-C and supplemental Videos 2-5). B-cell motility was completely abolished at high p31 densities (100 molecules/μm²); only a few cells moved and did so at low speed, describing very short tracks independently of the presence of CXCL13. Five times less p31 (20 molecules/μm²) allowed 30% of the B cells to migrate, but at approximately half the average speed and with tiny tracks. This motility was due mainly to CXCL13 signals, because p31 alone promoted some migration in only 10% of B cells. B-cell migration was recovered at low p31 densities (4 molecules/μm²), although with significant differences in average speed and cell tracks relative to controls (no p31).

To confirm our results in a different BCR-transgenic model and with another antigen, we used MD4 BCR-transgenic B cells that recognize HEL with very high affinity (K_A 5 × 10^{10} M^{-1}; see "Methods"). MD4 B cells migrated on ICAM-1–containing membranes in response to CXCL13, although in lower numbers and at a lower average speed than wild-type B cells (supplemental Figure 1A-C). Results were nonetheless similar to those obtained above. Because of the higher affinity and consequent stronger BCR signaling, MD4 B-cell migration stopped at 20 molecules/μm² antigen density. As HEL decreased (4 and 1 molecule/μm²), the CXCL13 signal overcame the BCR signaling effect and promoted migration of a percentage of the B-cell population (33% and 66%, respectively, of migration in the absence of antigen). These cells nonetheless moved more slowly and had short tracks (supplemental Figure 1A-C). To verify that the moving cells detected the low HEL density, we analyzed the levels of phosphorylated Syk (p-Syk), an early marker of BCR signaling,[21] at the B-cell contact zone with the membrane (see "Methods"). We costained with phalloidin, which identifies migratory cells by the lack of the F-actin ring characteristic of stopped cells that form an immune synapse.[22] Quantitative analyses of p-Syk fluorescence showed higher p-Syk levels in migratory MD4 B cells on CXCL13-coated membranes containing low doses of HEL than on membranes with chemokine alone (supplemental Figure 1D). Results were similar for 3-83 B cells in the presence of low p31 doses (not shown).

Our data indicate that BCR signaling strength, which is a direct function of abundance of and BCR affinity for antigen, models CXCL13-mediated B-cell migration with a wide range of consequences. Whereas strong BCR signals drive the B cell to halt its movement (STOP signal), weak BCR signals allow B cells to migrate in response to CXCL13 (GO signal) at frequencies near those of no antigen. A heterogeneous pattern of B-cell behaviors (lower migration frequency, diminished velocity, and shorter tracks) lies between the STOP and GO states.

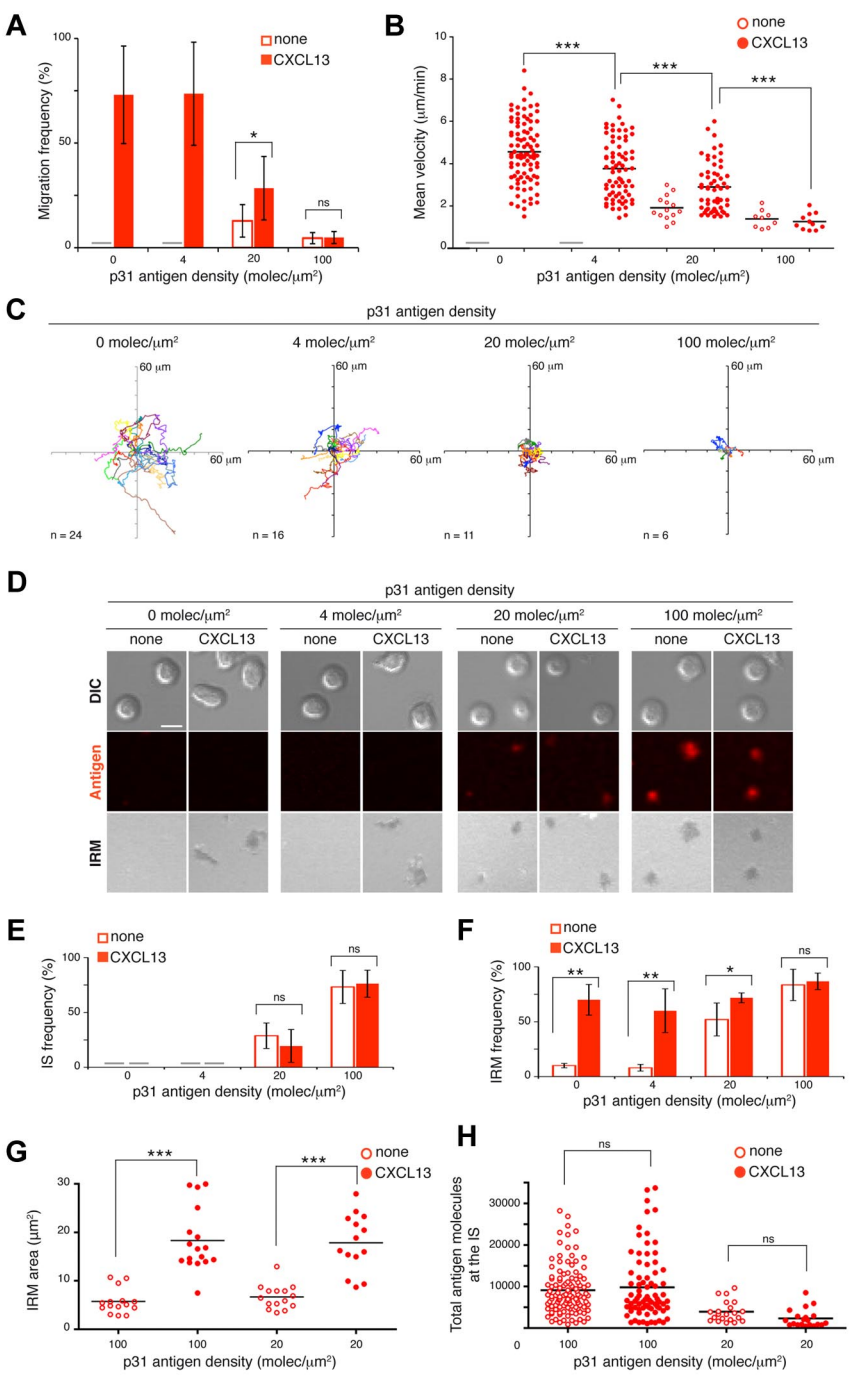

Figure 2. B-cell migration and IS formation in response to CXCL13 and antigen stimuli. Frequency of migration (A) and mean velocity (B) of 3-83 B cells on membranes with tethered p31 at different densities alone or with CXCL13. (C) Tracks of migratory 3-83 B cells in the presence of tethered p31 at the specified densities with CXCL13. (D) Representative DIC, fluorescent antigen, and IRM images at 30 minutes of naive 3-83 B cells settled on membranes bearing p31 at the indicated densities alone or with CXCL13. Scale bar indicates 5 μm. Frequency of IS formation estimated by fluorescence (E) and frequency (F) and area of B cell: membrane contacts estimated by IRM (G) 30 minutes after 3-83 B cells settling on membranes. (H) Total antigen molecules accumulated at the 3-83 IS established after 30 minutes on membranes with tethered p31 at the indicated densities alone or with CXCL13. All experiments were performed in the presence of ICAM-1 (150 molecules/μm²). Data in panels A, E, and F represent the means ± SEM of 4 experiments; data in panels B, C, and H correspond to the merge of 3 experiments; data of a representative experiment are shown in panel G. Gray bar indicates not detected; ns, not significant. $^*P < .05$; $^{**}P < .001$; $^{***}P < .0001$.

CXCL13/CXCR5 signaling does not interfere with BCR-triggered IS formation

To analyze BCR-promoted B-cell IS formation in the presence of CXCL13, we used confocal microscopy to follow the fluorescent signal of tethered antigen (Figure 2D and supplemental Videos 2-5). B-cell synapse formation was inversely correlated with CXCL13-induced B-cell migration. At a p31 density of 100 molecules/μm², nearly all 3-83 B cells formed a detectable IS as measured by antigen accumulation and formation of a central cluster (Figure 2D-E). This observation was correlated with a high frequency of B cell:membrane contacts (detected by IRM), which were CXCL13 independent (Figure 2F). At a 5-fold lower antigen density, only 20%-30% of 3-83 B cells showed measurable aggregation of p31; however, 75% of the cells were IRM positive in the presence of CXCL13 and 50% were in its absence (Figure 2E-F). The IRM areas were larger in the presence of CXCL13 than in its absence at both p31 densities (Figure 2G). We detected no IS at a p31 density of 4 molecules/μm², although LFA-1 was active on the 3-83 B-cell surface in the presence of CXCL13 (~ 70% of B cells were IRM positive; Figure 2E-F). There were no significant differences in the total number of p31 molecule at the IS using antigen alone or with CXCL13 (Figure 2G). Results were similar for MD4 B cells and the high-affinity HEL antigen (supplemental Figure 1E-H).

Our data indicate that CXCL13/CXCR5 signaling does not significantly affect the frequency of BCR-triggered B cells that

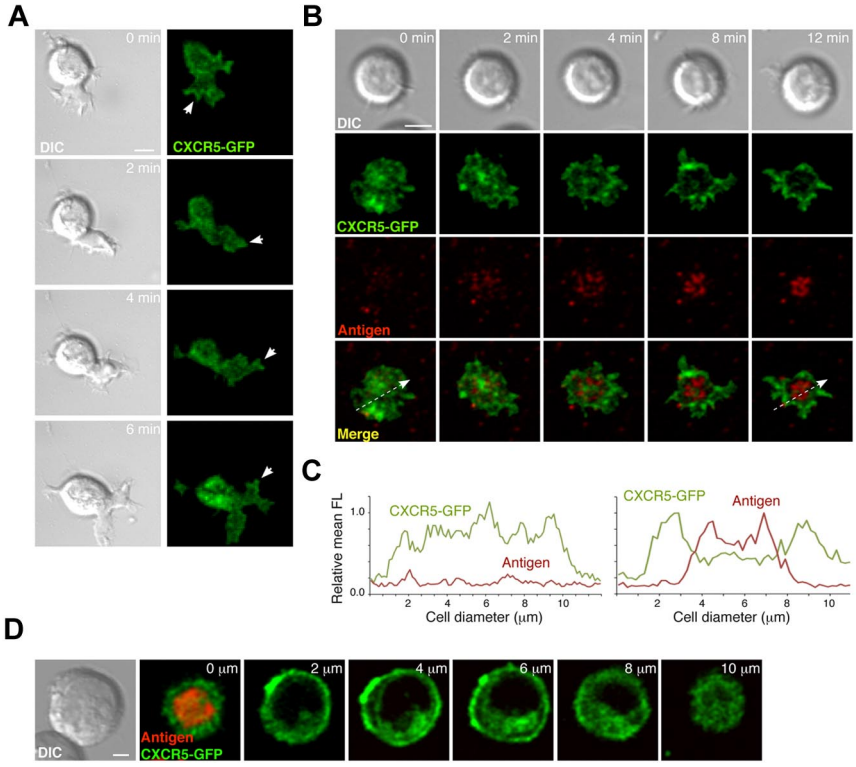

Figure 3. CXCR5 distribution at the contact site of migratory B cells and at the B-cell IS. (A) Representative DIC and fluorescence images at the contact site of a typical migratory A20 B cell in the absence of tethered antigen at the indicated times. White arrows indicate aggregates of CXCR5-GFP at the tips of the leading edge. Scale bar indicates 5 μm. (B) DIC and fluorescent images of a representative A20 B cell forming the IS after surrogate antigen (anti-κ mAb) recognition on the membrane. Scale bar indicates 5 μm. (C) Profiles of relative mean fluorescence distribution of CXCR5-GFP (green line) and antigen (red line) at the contact site of the A20 B cell with the membrane at 0 minutes (left; white arrow at bottom left panel in B) and 12 minutes (right; white arrow at bottom right panel in B). (D) Serial *z*-stack sections taken every 2 μm of a representative A20 B cell with an established IS on membranes with tethered surrogate antigen. Scale bar indicates 2 μm. All experiments were performed in the presence of ICAM-1 (150 molecules/μm^2).

establish an IS or the quantity of antigen accumulated at the IS. By promoting the LFA-1/ICAM-1 interaction, CXCL13/CXCR5 signaling nonetheless enhances the frequency and/or area of contact with the membrane.

CXCR5 is excluded from the cSMAC but does not polarize to the B-cell IS

To study the molecular dynamics of CXCR5 at the B cell:target membrane interface in the migratory stage compared with IS formation, we generated the CXCR5-GFP construct and transfected it into the A20 B-cell line; we then used confocal microscopy to follow CXCR5-GFP distribution at the B cell:membrane interface through time. Contact with CXCL13-coated ICAM-1–containing membranes promoted movement in 15%-20% of A20 B cells (data not shown), in which CXCR5-GFP was distributed homogenously at the contact zone, with some aggregates at the tips of the leading cell edge (Figure 3A and supplemental Video 6). In contact with membranes that included tethered surrogate antigen (anti-κ mAb; see "Methods"), CXCR5-GFP segregated to the periphery of the contact zone, whereas antigen accumulated at the center to form the so-called central supramolecular activation cluster (cSMAC; Figure 3B-C and supplemental Video 6). Analysis of the GFP signal in the remainder of the cell body nevertheless indicated that CXCR5-GFP did not polarize to the IS (Figure 3D). To confirm these data in primary naive B cells, we immunostained fixed cells and used confocal microscopy to analyze endogenous CXCR5 distribution in conjugates of 3-83 B cells with antigen-presenting cells (ICAM-1-GFP transfectants of L cells expressing H-2K^K, an antigen recognized by the 3-83 BCR; see "Methods"). Three-dimensional reconstruction of confocal images at the IS site showed CXCR5 exclusion from the cSMAC, whereas it colocalized with the distinctive ICAM-1 ring of the peripheral SMAC (pSMAC; supplemental Figure 2); again, we observed no CXCR5 polarization to the B-cell IS; the chemokine receptor remained evenly distributed over the remainder of the B-cell surface.

Our results show that whereas the B cell migrates, CXCR5 distribution is relatively homogenous on the area of contact with the target cell. Antigen recognition through the BCR triggers IS formation; CXCR5 subsequently segregates toward the periphery of the contact zone and is excluded from the cSMAC but not from the pSMAC. Nevertheless, CXCR5 does not polarize to the target cell contact site in the B-cell synaptic phase.

CXCL13/CXCR5 signaling enhances BCR-mediated B-cell activation

To determine the effect of CXCL13 in the process of B-cell activation by antigen, we cultured naive MD4 B cells (18-20 hours) on membranes bearing different densities of tethered HEL alone or with chemokine. Cells were collected and CD86 and CD69 activation marker expression analyzed at the B-cell surface by flow cytometry (Figure 4). We found a significant increase in the frequency of B-cell activation (CD86^{hi}CD69$^+$) in the presence of CXCL13 at HEL densities of 4 and 1 molecule/μm^2 (conditions in which no IS was detected and a fraction of B cells migrated; supplemental Figure 1). No significant chemokine effect was detected at 20 molecules/μm^2. Results were similar for naive 3-83 B cells and p31 (supplemental Figure 3A).

To confirm that enhanced B-cell activation was due to CXCL13 signaling through CXCR5, we carried out activation assays using naive B cells isolated from wild-type and CXCR5-deficient mice. Membrane-bound anti-κ mAb was used as a surrogate antigen because these cells were not BCR transgenic; we focused on low antigen densities at the membrane to improve detection of the chemokine effect. Whereas CXCL13 increased wild-type B-cell activation in response to the surrogate antigen, no effect was

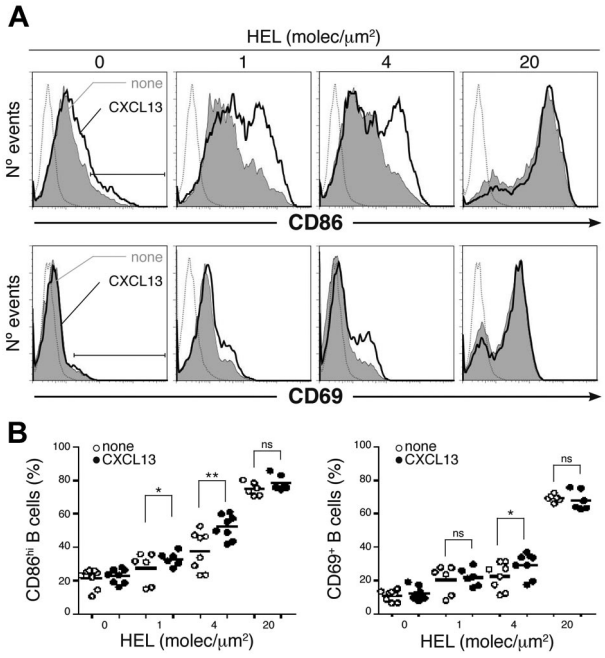

Figure 4. CXCL13/CXCR5 signaling effect on B-cell activation by antigen. (A) CD86 (top panels) and CD69 (bottom panels) profiles of a representative experiment of MD4 B cells settled on membranes with tethered HEL at the specified densities alone (gray filled histogram) or with CXCL13 (black line). Dashed gray line is the isotype control; black bar, CD86^{hi} and CD69^{+} B cells. (B) Frequency of CD86^{hi} (left panel) and CD69^{+} (right panel) MD4 B cells in the same conditions as in panel A; dots represent single experiments; black horizontal bars, averaged values. All experiments were performed in the presence of ICAM-1 (150 molecules/μm^2). ns indicates not significant. *$P < .05$; **$P < .001$.

observed on CXCR5-deficient B cell activation at any antigen density tested (supplemental Figure 3B).

We conclude that CXCL13/CXCR5 signaling boosts BCR-mediated B-cell activation. This effect is more robust in limiting conditions of BCR stimulation (low antigen abundance).

CXCL13/CXCR5 signaling assists antigen gathering at the B-cell IS by promoting membrane ruffling and LFA-1–supported contact

We studied the molecular mechanism underlying the CXCL13/CXCR5–mediated increase in antigen activation of B cells. We observed enhanced frequency and area of B cell:target membrane contacts when CXCL13 was present (Figure 2F-G and supplemental Figure 1G-H); therefore, CXCR5 signaling promoted LFA-1/ICAM-1 interactions. This pair of adhesion molecules facilitates antigen-mediated B-cell activation by mediating adhesion and IS formation.[6] We focused on the membrane contacts established by halted B cells (IS stage); the presence of CXCL13 supported dynamic contact over time, with constant changes in shape and area as determined by IRM (Figure 5A, supplemental Videos 7 and 8, and supplemental Figure 4A). Establishment of new contacts coincided with the detection of membrane ruffles extension by DIC, and was usually accompanied by detectable antigen gathering from the area near the IS toward the cSMAC (measured by fluorescence; Figure 5A and supplemental Figure 4A). CXCL13-mediated enhancement of membrane ruffling on halted B cells was detected at all antigen densities tested (Figure 5B and supplemental Figure 4B), and was also observed in the absence of antigen on the

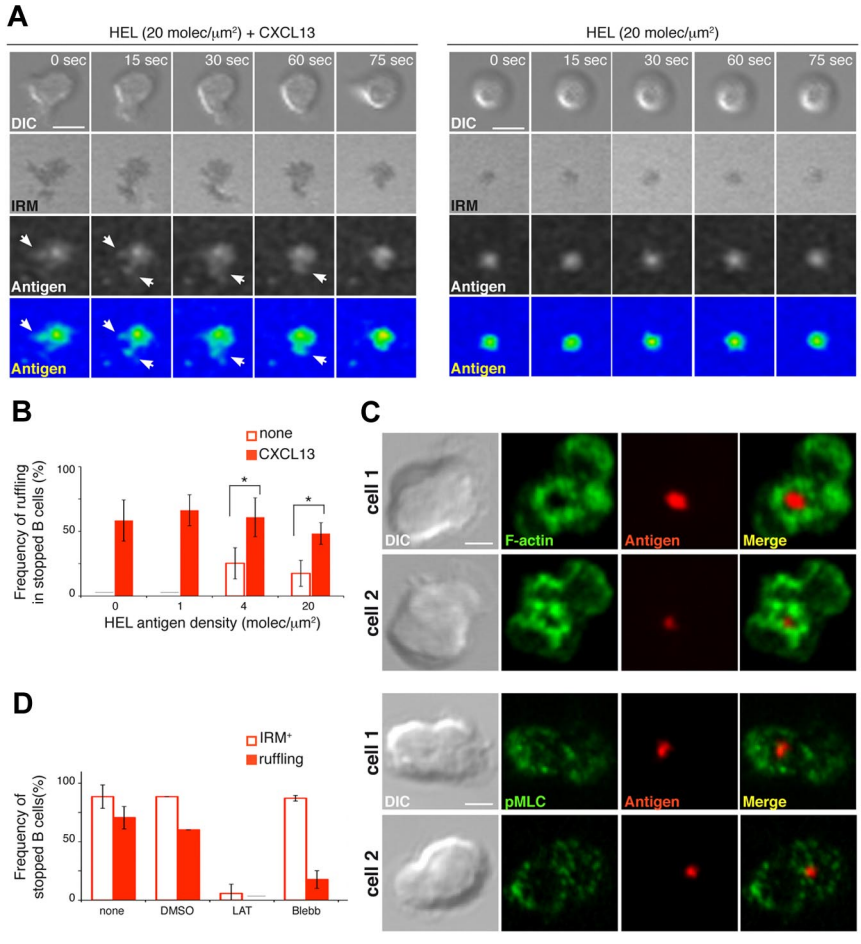

Figure 5. CXCL13/CXCR5 signaling promotes membrane ruffling and LFA-1–supported contacts to enhance antigen gathering at the B-cell IS. (A) Time-lapse DIC, IRM, and fluorescence antigen images (in gray scale and color-coded scale) of representative MD4 B cells on membranes with tethered HEL (20 molecules/μm^2) alone or with CXCL13. White arrows indicate monitored antigen gathering. Scale bar indicates 5 μm. (B) Proportion of halted MD4 B cells showing membrane ruffles on membranes bearing HEL at the specified density alone and with CXCL13. (C) DIC and fluorescent images for antigen, F-actin, and pMLCs of 2 representative fixed MD4 B cells in each case on CXCL13-coated membranes tethered with HEL (20 molecules/μm^2). Scale bar indicates 2 μm. (D) Frequency of stopped MD4 B cells that show target membrane contact (IRM^{+}) and extend ruffles (estimated by DIC) on CXCL13-coated membranes with tethered HEL after treatment with 0.1% DMSO (carrier), 0.5μM latrunculin A (LAT), 50μM blebbistatin (Blebb), or no treatment (none). All experiments were performed in the presence of ICAM-1 (150 molecules/μm^2). Data in panels B and D represent the mean ± SEM of 4 experiments. Gray bar indicates not detected. *$P < .05$.

few halted B cells found. The absence of ICAM-1 prevented contact of the CXCL13-triggered ruffle with the target membrane and therefore antigen gathering from the synapse vicinity (supplemental Figure 4C-D). Similar studies of wild-type compared with CXCR5-deficient B cells confirmed that this effect requires CXCR5 signaling (supplemental Figure 5).

F-actin analysis by phalloidin staining on fixed B cells showed actin cytoskeleton reorganization at the CXCL13-mediated membrane ruffles, in addition to the classic F-actin ring that surrounds the antigen cluster at the IS (Figure 5C). Once IS were established, the addition of latrunculin A (a drug that inhibits actin polymerization) to planar lipid bilayers completely abolished membrane ruffling on halted B cells, also leading to their detachment from the target membrane within minutes (Figure 5D). Membrane ruffle extension was followed by its contraction to the cell body, which led us to target NM-II, a motor protein that exerts contraction of actin filaments.[23] NM-II function requires phosphorylation of the regulatory myosin light chains (MLCs). Using immunofluorescence techniques, we detected phosphorylated MLCs (pMLCs) at the B-cell contact area with the target membrane (Figure 5C). pMLCs showed patched distribution in the vicinity of the B-cell IS antigen cluster, but associated mainly with the outer edges of the cell. Therefore, these data suggested the presence of active NM-II at the membrane ruffles. Treatment of halted B cells with the specific NM-II inhibitor blebbistatin blocked CXCL13-mediated membrane ruffling within minutes; halted B cells nonetheless remained adhered to the target membrane (Figure 5D).

Our data show that CXCL13/CXCR5 signaling enhances BCR-mediated B-cell activation by assisting antigen gathering from the IS surroundings through membrane ruffling and LFA-1–supported contacts with the target membrane. Both events depend on a functional actin cytoskeleton and NM-II motor protein activity.

CXCL13-mediated migration allows BCR signal integration through establishment of an LFA-1–supported migratory junction or kinapse

CXCL13-mediated enhancement of membrane contacts detected at low antigen densities (p31 density of 4 molecules/μm^2; HEL density of 1 molecule/μm^2) was correlated with high cell migration frequency (Figure 2A, F and supplemental Figure 1A, G). Several studies indicated that T cells integrate antigen/TCR-mediated signals while migrating over the surface of the antigen-presenting cell,[24-26] and this migratory junction is called a kinapse.[27] We studied this possibility on migratory B cells as an additional mechanism for the CXCL13/CXCR5–mediated increase in BCR-mediated B-cell activation. To track BCR signaling, we monitored Ca^{2+} flux in MD4 B cells in contact with membranes bearing HEL at a density of 1 molecule/μm^2 alone or with CXCL13. B cells were preloaded with Fluo4FF and Ca^{2+} changes were followed by real-time confocal microscopy; we detected intermittent Ca^{2+} signals in half of the migratory B cells on CXCL13-coated target membranes (Figure 6A-B and supplemental Video 9). There were no measurable changes in Ca^{2+} levels on B cells settled on target membranes in the absence of chemokine (Figure 6A) or in the absence of ICAM-1 (not shown); in both conditions, cells floated above the membrane due to lack of contact (supplemental Figures 1G and 6D). In the presence of CXCL13, we also detected Ca^{2+} signals on migratory B cells at 4 molecules/μm^2 HEL or even with no antigen (Figure 6B). Chemokine receptors trigger Ca^{2+} influx after ligand binding[28]; however, single-cell Ca^{2+} profiles showed higher intensity peaks when antigen was available than with chemokine alone at the target membrane (Figure 6C). Results were similar for 3-83 B cells (supplemental Figure 6A-C).

We used immunofluorescence techniques to analyze the actomyosin network on migratory B cells at the contact zone with the target membrane. Phalloidin staining indicated actin cytoskeleton rearrangement at the leading edge; pMLCs showed a patched pattern across the entire contact area, with brightest signals near the border (Figure 6D). Latrunculin A inhibition of actin polymerization on migratory B cells eliminated cell motility within minutes, as well as adhesion to the ICAM-1–containing target membrane (Figure 6E). Blebbistatin treatment of migratory B cells to inhibit NM-II eradicated cell motility, but not LFA-1–supported membrane contact (Figure 6E).

Our data indicated that at antigen densities unable to promote B-cell stop and IS formation, CXCL13-mediated migration allows antigen encounter and integration of BCR signals by establishing an LFA-1–supported kinapse, and this process requires operative actin cytoskeleton and NM-II motor protein. Through this mechanism, CXCR5 signaling could also enhance BCR-mediated B-cell activation.

Discussion

In the present study, we sought to understand the interplay between 2 ligand/receptor pairs involved in B-cell dynamics at the follicle, CXCL13/CXCR5 and antigen/BCR, and to determine how B-cell fate could be affected by instructing cell behavior. We established a 2-dimensional model based on ICAM-1–containing planar membranes, in which naive B cells move in response to a CXCL13 coating. The migration pattern resembles the in vivo dynamics of B cells on the FDC network in lymph nodes (random tracks, average speed ~ 6 μm/min). The combination of CXCL13 and antigen stimulation at the membrane results in a wide range of B-cell behaviors based on BCR signaling strength. We observed that CXCL13/CXCR5 signaling did not impair BCR-triggered B-cell IS formation; however, it significantly enhanced BCR-mediated B-cell activation. The presence of CXCL13 led to markedly increased membrane ruffling and LFA-1–supported adhesion in halted/IS-forming B cells; both events assisted antigen gathering from the synapse vicinity and thus BCR signaling. At limiting conditions of antigen abundance, CXCL13-mediated migration promoted the formation of an LFA-1–supported kinapse that allowed antigen encounter and BCR signaling events (Ca^{2+} influx) on motile B cells. Through these 2 means, dependent on a functional actomyosin network, CXCR5 signaling boosts BCR-mediated B-cell activation.

Our data showed modulation of CXCL13-mediated B-cell migration by integrin ligand density at the target membrane. We found ICAM-1 densities of 100-200 molecules/μm^2 on the surface of splenocytes in steady state (not shown; see supplemental Methods). After inflammatory stimulation, adhesion molecule expression increased at the surface of different cell types (after 20 hours of in vitro TNF stimulation, splenocytes expressed ICAM-1 densities of > 600 molecules/μm^2; data not shown). These changes in the environment could retard B-cell movement in vivo, promoting a more meticulous search for antigen. Although leukocyte movement can occur in the absence of integrins,[29] the same investigators recently described a cell preference for movement over a surface with an ICAM-1 and a chemokine coating (haptokinesis), even when chemotactic signals were present.[20] Adhesion molecule levels and possibly their distribution pattern,[30]

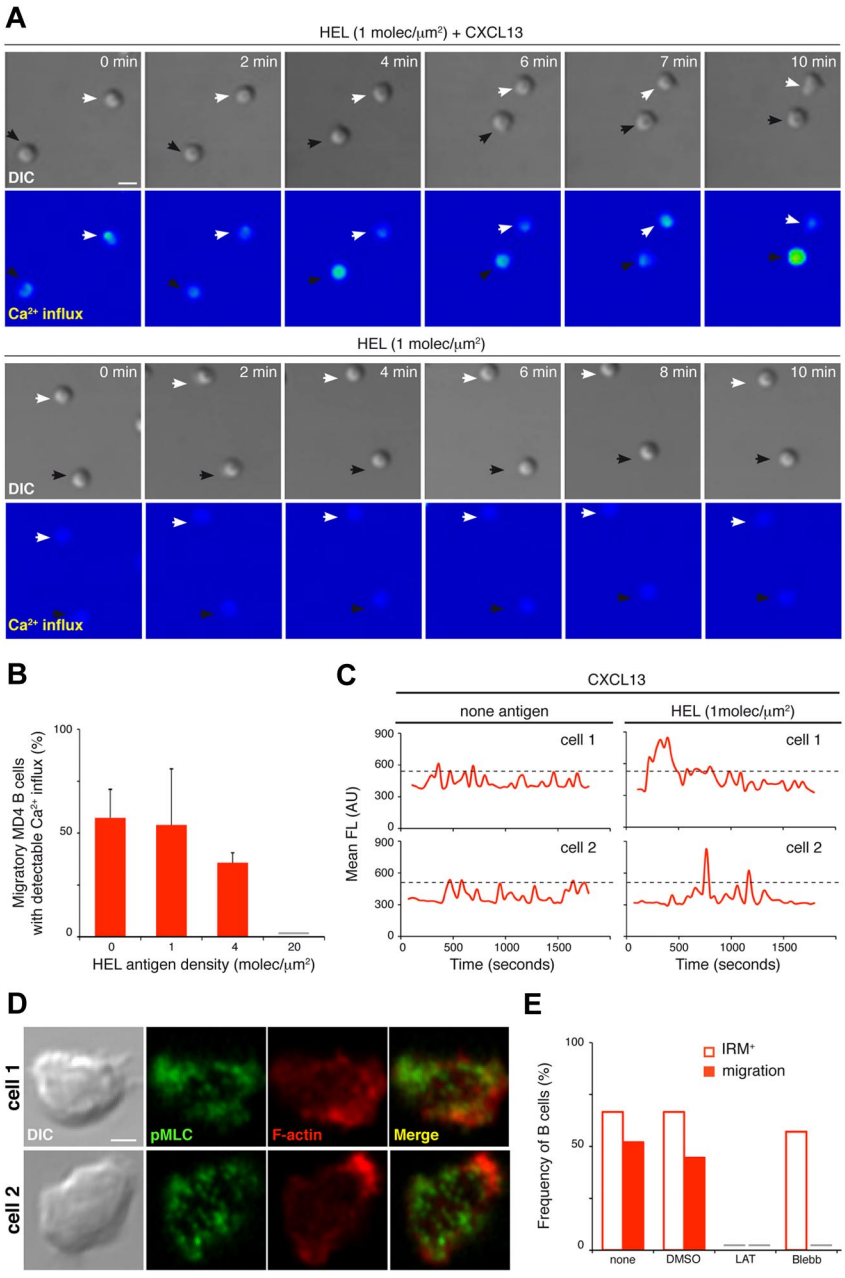

Figure 6. CXCL13/CXCR5 signaling establishes an LFA-1–supported kinapse to facilitate BCR signal integration on motile B cells. (A) Time-lapse DIC and fluorescence images (Ca^{2+} influx, color-coded scale) of representative MD4 B cells on membranes with tethered HEL (1 molecule/μm^2) alone or with CXCL13. White and black arrows identify B cells monitored in each condition. Scale bar indicates 5 μm. (B) Proportion of migratory MD4 B cells showing Ca^{2+} influx on membranes bearing HEL at the specified density and with CXCL13; data represent the means ± SEM of 4 experiments. (C) Ca^{2+} influx profiles of single migratory MD4 B cells on CXCL13-coated membranes with no antigen or tethered HEL (1 molecule/μm^2). Profiles of 2 representative cells are shown in each case; dashed black line indicates maximum Ca^{2+} signal for only chemokine stimuli. (D) DIC and fluorescent images for F-actin (red) and pMLC (green) of 2 representative fixed MD4 B cells on CXCL13-coated membranes in the absence of antigen. Scale bar indicates 2 μm. (E) Frequency of B cells that show target membrane contact (IRM^+) and migration (estimated by DIC) on CXCL13-coated membranes in the absence of antigen after treatment with 0.1% DMSO (carrier), 0.5μM latrunculin A (LAT), 50μM blebbistatin (Blebb), or no treatment (none); data of one representative experiment are shown. Gray bar indicates not detected. All experiments were performed in the presence of ICAM-1 (150 molecules/μm^2).

as well as chemokine-regulated integrin adhesiveness,[19] thus appear to be pivotal factors in the modulation of interstitial leukocyte dynamics, which remains to be explored in depth.

Few studies have addressed the molecular dynamics of chemokine receptors at the IS. In T cells, CXCR4 and CCR5 are recruited to the IS[31]; specifically, CXCR4 appears to localize at the pSMAC.[32] Our study establishes CXCR5 distribution at the B-cell synapse. CXCR5 localization at the pSMAC could help to promote membrane ruffling at the synaptic stage; in addition, its nonpolarization to the IS might maintain B cells' ability to respond to CXCL13 in the vicinity of the target cell. During B-cell migration, CXCR5 is distributed nearly homogeneously at the target membrane contact site. Although we detected some receptor aggregates or clusters at the leading edge tips, CXCR5 did not polarize, as suggested for other chemokine receptors.[33,34] Relatively uniform CXCR5 distribution at the contact site could help to explain the rapid, random changes in direction during B-cell migration.

Our results identify a costimulatory function for CXCL13/CXCR5 signaling in BCR-triggered B-cell activation; this effect was more pronounced in suboptimal BCR stimulation conditions. We found that the CXCR5-mediated effect on cell dynamics assists BCR-triggered B-cell activation. At limiting conditions of antigen density, naive B cells established an LFA-1–supported kinapse with the target membrane in response to CXCL13; through this migratory junction, they encountered antigen and integrated BCR signals. When antigen density was sufficient to trigger a stop signal through the BCR, naive B cells established a synapse with the target membrane; CXCR5 signaling then promoted membrane ruffling and LFA-1/ICAM-1 contacts that increased antigen gathering near the IS and thus BCR signaling. Other studies have highlighted the importance of cell behavior modulation for lymphocyte fate. APC-bound CCL21 appears to prime T cells for IS formation.[35] CXCR4 and CCR5 promote more stable T cell:APC

conjugates by increasing adhesion.[31] Chemokine-guided recruitment of CD8 T cells to CD4 T cell/dendritic cell interaction sites fosters generation of memory CD8 T cells.[36] Regulation of thymocyte dynamics also appears to be critical for positive selection events in the thymus.[37] In any case, we cannot discard a role for CXCR5-mediated activation of other signaling pathways in costimulation, and further studies are clearly needed.

The actomyosin network has a critical role in cell polarization, migration, and adhesion. In T cells, NM-II is necessary for fast ameboid motility; this motor protein regulates surface contact area to allow high speed of movement.[38-40] NM-II is also important for the formation and persistence of T-cell synapses and for TCR signaling.[41] In B cells, this motor protein is needed for BCR-driven antigen processing and presentation.[42] Our immunofluorescence and drug-treatment data also suggest participation by and the necessity for an operative actomyosin network for CXCL13-mediated, LFA-1–supported B-cell motility and membrane ruffling. At longer treatment times, NM-II inhibition also provoked disassembly of the antigen cluster at the B-cell synapse (not shown).

The detection of antigen/BCR early signaling (Ca^{2+} flux) during B-cell migration led us to question the need to establish an immune synapse for B-cell activation. Several studies in T cells have indicated TCR signal integration during migration in response to chemokines[24,25]; the moving cell-cell junction that permits signal integration was defined as the kinapse.[27] Recent in vivo studies showed antigen-triggered TCR internalization in the absence of T-cell arrest; the investigators proposed a flexible relationship between motility and the immune synapse, and that successful signaling does not necessarily require cSMAC formation.[43] Based on our data, we propose that B cells also exploit both types of interfaces, kinapses and synapses, to integrate BCR signals, with the use of one or the other being determined mainly by antigen quality and abundance. In T cells, PKCθ and WASp proteins regulate kinapse/synapse interconversion.[44] We have not observed this interconversion in our assays; nonetheless, further studies will lead to a better comprehension of this phenomenon in B-cell dynamics.

Acknowledgments

The authors thank F. Batista, E. Fernández, S. Minguet, I. Moreno de Alborán, and L. Planelles for critical reading of the manuscript and C. Mark for editorial assistance.

This work was supported by grants from the European Union (FP7-integrated project Masterswitch 223404 FP7) and from the Spanish Ministry of Science (BFU2008-01194). J.S. is supported by a contract from the Comunidad Autónoma de Madrid. Y.R.C. is supported by a Ramón y Cajal contract from the Spanish Ministry of Science.

Authorship

Contribution: J.S.d.G. designed parts of the study, performed the experiments, analyzed the data, and assisted in manuscript preparation; L.B. performed some of the experiments, analyzed the data, and assisted in manuscript preparation; M.M. provided input into the project; and Y.R.C. designed and supervised all aspects of the work and wrote the manuscript.

Conflict-of-interest disclosure: The authors declare no competing financial interests.

Correspondence: Yolanda R. Carrasco, B Cell Dynamics Group, Department of Immunology and Oncology, Centro Nacional de Biotecnología/CSIC, Darwin 3, UAM Campus Cantoblanco, Madrid E-28049 Spain; e-mail: ycarrasco@cnb.csic.es.

References

1. Miller MJ, Wei SH, Parker I, Cahalan MD. Two-photon imaging of lymphocyte motility and antigen response in intact lymph node. *Science.* 2002;296(5574):1869-1873.
2. Okada T, Miller MJ, Parker I, et al. Antigen-engaged B cells undergo chemotaxis toward the T zone and form motile conjugates with helper T cells. *PLoS Biol.* 2005;3(6):e150.
3. Bajénoff M, Egen JG, Koo LY, et al. Stromal cell networks regulate lymphocyte entry, migration, and territoriality in lymph nodes. *Immunity.* 2006; 25(6):989-1001.
4. Allen CD, Cyster JG. Follicular dendritic cell networks of primary follicles and germinal centers: phenotype and function. *Semin Immunol.* 2008; 20(1):14-25.
5. Carrasco YR, Batista FD. B cells acquire particulate antigen in a macrophage-rich area at the boundary between the follicle and the subcapsular sinus of the lymph node. *Immunity.* 2007; 27(1):160-171.
6. Carrasco YR, Fleire SJ, Cameron T, Dustin ML, Batista FD. LFA-1/ICAM-1 interaction lowers the threshold of B cell activation by facilitating B cell adhesion and synapse formation. *Immunity.* 2004;20(5):589-599.
7. Fleire SJ, Goldman JP, Carrasco YR, Weber M, Bray D, Batista FD. B cell ligand discrimination through a spreading and contraction response. *Science.* 2006;312(5774):738-741.
8. Randall KL, Lambe T, Johnson A, et al. Dock8 mutations cripple B cell immunological synapses, germinal centers and long-lived antibody production. *Nat Immunol.* 2009;10(12):1283-1291.
9. Goodnow CC, Crosbie J, Adelstein S, et al. Altered immunoglobulin expression and functional silencing of self-reactive B lymphocytes in transgenic mice. *Nature.* 1988;334(6184):676-682.
10. Russell DM, Dembic Z, Morahan G, Miller JF, Burki K, Nemazee D. Peripheral deletion of self-reactive B cells. *Nature.* 1991;354(6351):308-311.
11. Förster R, Mattis AE, Kremmer E, Wolf E, Brem G, Lipp M. A putative chemokine receptor, BLR1, directs B cell migration to defined lymphoid organs and specific anatomic compartments of the spleen. *Cell.* 1996;87(6):1037-1047.
12. Kouskoff V, Famiglietti S, Lacaud G, et al. Antigens varying in affinity for the B cell receptor induce differential B lymphocyte responses. *J Exp Med.* 1998;188(8):1453-1464.
13. Grakoui A, Bromley SK, Sumen C, et al. The immunological synapse: a molecular machine controlling T cell activation. *Science.* 1999; 285(5425):221-227.
14. Cyster JG, Ansel KM, Reif K, et al. Follicular stromal cells and lymphocyte homing to follicles. *Immunol Rev.* 2000;176:181-193.
15. de Paz JL, Moseman EA, Noti C, Polito L, von Andrian UH, Seeberger PH. Profiling heparin-chemokine interactions using synthetic tools. *ACS Chem Biol.* 2007;2(11):735-744.
16. Koopman G, Parmentier HK, Schuurman HJ, Newman W, Meijer CJ, Pals ST. Adhesion of human B cells to follicular dendritic cells involves both the lymphocyte function-associated antigen 1/intercellular adhesion molecule 1 and very late antigen 4/vascular cell adhesion molecule 1 pathways. *J Exp Med.* 1991;173(6):1297-1304.
17. Dustin ML. Cell adhesion molecules and actin cytoskeleton at immune synapses and kinapses. *Curr Opin Cell Biol.* 2007;19(5):529-533.
18. Smith A, Stanley P, Jones K, Svensson L, McDowall A, Hogg N. The role of the integrin LFA-1 in T-lymphocyte migration. *Immunol Rev.* 2007;218:135-146.
19. Woolf E, Grigorova I, Sagiv A, et al. Lymph node chemokines promote sustained T lymphocyte motility without triggering stable integrin adhesiveness in the absence of shear forces. *Nat Immunol.* 2007;8(10):1076-1085.
20. Schumann K, Lammermann T, Bruckner M, et al. Immobilized chemokine fields and soluble chemokine gradients cooperatively shape migration patterns of dendritic cells. *Immunity.* 2010; 32(5):703-713.
21. Johnson SA, Pleiman CM, Pao L, Schneringer J, Hippen K, Cambier JC. Phosphorylated immunoreceptor signaling motifs (ITAMs) exhibit unique abilities to bind and activate Lyn and Syk tyrosine kinases. *J Immunol.* 1995;155(10):4596-4603.
22. Arana E, Vehlow A, Harwood NE, et al. Activation of the small GTPase Rac2 via the B cell receptor regulates B cell adhesion and immunological-synapse formation. *Immunity.* 2008;28(1):88-99.
23. Vicente-Manzanares M, Ma X, Adelstein RS, Horwitz AR. Non-muscle myosin II takes centre stage in cell adhesion and migration. *Nat Rev Mol Cell Biol.* 2009;10(11):778-790.
24. Underhill DM, Bassetti M, Rudensky A,

Aderem A. Dynamic interactions of macrophages with T cells during antigen presentation. *J Exp Med.* 1999;190(12):1909-1914.

25. Gunzer M, Schafer A, Borgmann S, et al. Antigen presentation in extracellular matrix: interactions of T cells with dendritic cells are dynamic, short lived, and sequential. *Immunity.* 2000;13(3):323-332.
26. Mempel TR, Henrickson SE, Von Andrian UH. T-cell priming by dendritic cells in lymph nodes occurs in three distinct phases. *Nature.* 2004; 427(6970):154-159.
27. Dustin ML. Hunter to gatherer and back: immunological synapses and kinapses as variations on the theme of amoeboid locomotion. *Annu Rev Cell Dev Biol.* 2008;24:577-596.
28. Thelen M, Stein JV. How chemokines invite leukocytes to dance. *Nat Immunol.* 2008;9(9):953-959.
29. Lämmermann T, Bader BL, Monkley SJ, et al. Rapid leukocyte migration by integrin-independent flowing and squeezing. *Nature.* 2008; 453(7191):51-55.
30. Barreiro O, Zamai M, Yanez-Mo M, et al. Endothelial adhesion receptors are recruited to adherent leukocytes by inclusion in preformed tetraspanin nanoplatforms. *J Cell Biol.* 2008;183(3):527-542.
31. Molon B, Gri G, Bettella M, et al. T cell costimulation by chemokine receptors. *Nat Immunol.* 2005; 6(5):465-471.
32. Pérez-Martínez M, Gordon-Alonso M, Cabrero JR, et al. F-actin-binding protein drebrin regulates CXCR4 recruitment to the immune synapse. *J Cell Sci.* 2010;123(pt 7):1160-1170.
33. Nieto M, Frade JM, Sancho D, Mellado M, Martinez AC, Sanchez-Madrid F. Polarization of chemokine receptors to the leading edge during lymphocyte chemotaxis. *J Exp Med.* 1997;186(1): 153-158.
34. Vicente-Manzanares M, Montoya MC, Mellado M, et al. The chemokine SDF-1alpha triggers a chemotactic response and induces cell polarization in human B lymphocytes. *Eur J Immunol.* 1998; 28(7):2197-2207.
35. Friedman RS, Jacobelli J, Krummel MF. Surface-bound chemokines capture and prime T cells for synapse formation. *Nat Immunol.* 2006;7(10): 1101-1108.
36. Castellino F, Huang AY, Altan-Bonnet G, Stoll S, Scheinecker C, Germain RN. Chemokines enhance immunity by guiding naive CD8+ T cells to sites of CD4+ T cell-dendritic cell interaction. *Nature.* 2006;440(7086):890-895.
37. Phee H, Dzhagalov I, Mollenauer M, et al. Regulation of thymocyte positive selection and motility by GIT2. *Nat Immunol.* 2010;11(6):503-511.
38. Jacobelli J, Chmura SA, Buxton DB, Davis MM, Krummel MF. A single class II myosin modulates T cell motility and stopping, but not synapse formation. *Nat Immunol.* 2004;5(5):531-538.
39. Jacobelli J, Bennett FC, Pandurangi P, Tooley AJ, Krummel MF. Myosin-IIA and ICAM-1 regulate the interchange between two distinct modes of T cell migration. *J Immunol.* 2009;182(4):2041-2050.
40. Jacobelli J, Friedman RS, Conti MA, et al. Confinement-optimized three-dimensional T cell amoeboid motility is modulated via myosin IIA-regulated adhesions. *Nat Immunol.* 2010;11(10): 953-961.
41. Ilani T, Vasiliver-Shamis G, Vardhana S, Bretscher A, Dustin ML. T cell antigen receptor signaling and immunological synapse stability require myosin IIA. *Nat Immunol.* 2009;10(5):531-539.
42. Vascotto F, Lankar D, Faure-Andre G, et al. The actin-based motor protein myosin II regulates MHC class II trafficking and BCR-driven antigen presentation. *J Cell Biol.* 2007;176(7):1007-1019.
43. Friedman RS, Beemiller P, Sorensen CM, Jacobelli J, Krummel MF. Real-time analysis of T cell receptors in naive cells in vitro and in vivo reveals flexibility in synapse and signaling dynamics. *J Exp Med.* 2010;207(12):2733-2749.
44. Sims TN, Soos TJ, Xenias HS, et al. Opposing effects of PKCtheta and WASp on symmetry breaking and relocation of the immunological synapse. *Cell.* 2007;129(4):773-785.